Stage-specific expression patterns and co-targeting relationships among miRNAs in the developing mouse cerebral cortex

Hristo Todorov[1], Stephan Weißbach[1,2], Laura Schlichtholz[1,3], Hanna Mueller[1], Dewi Hartwich[1], Susanne Gerber[*1], Jennifer Winter[*1,4]

[1] Institute of Human Genetics, University Medical Center of the Johannes Gutenberg University Mainz, Germany

[2] Institute of Developmental Biology and Neurobiology (iDN), Johannes Gutenberg University, Mainz, Germany

[3] Focus Program of Translational Neurosciences, University Medical Center Mainz, Mainz, Germany

[4] Lead contact: Jennifer Winter

[*] Corresponding authors: Susanne Gerber and Jennifer Winter

Contact data

Hristo Todorov: hristo.todorov@uni-mainz.de

Stephan Weißbach: s.weissbach@uni-mainz.de

Laura Schlichtholz: schlichtholz.laura@googlemail.com

Hanna Mueller: hanna.mueller.1909@gmail.com

Dewi Hartwich: dewi.hartwich@unimedizin-mainz.de

Susanne Gerber: sugerber@uni-mainz.de

Jennifer Winter: jewinter@uni-mainz

Keywords

Embryonic cortical development, miRNAs, co-targeting networks, gene silencing

Abstract

Background: microRNAs are a class of small RNAs that induce transcriptional inhibition via binding to the 3'-untranslated region (3'UTR) of their target mRNAs. In addition to other developmental processes, miRNAs are particularly important during brain development. However, the composition and temporal dynamics of miRNA regulatory networks are not yet sufficiently characterized.

Results: We performed small RNA sequencing of mouse embryonic cortical samples at E14, E17, and P0 as well as in neural progenitor cells (NPCs) differentiated *in vitro* into neurons. Using co-expression network analysis, we detected clusters of miRNAs that were co-regulated at distinct developmental stages with miRNAs such as miR-92a/b acting as hubs during early and miR-124 and miR-137 during late neurogenesis. Notably, the validated targets of hub miRNAs up-regulated at P0 were significantly enriched for genes down-regulated at this time point. These targets included important mediators of alternative splicing which is a crucial process during neuronal differentiation. In a co-targeting network of miRNAs sharing more targets than expected by chance, we observed that more abundant miRNAs were significantly associated with more co-targeting associations. Using luciferase reporter assays, we demonstrated that simultaneous binding of miRNA pairs to neurodevelopmentally relevant genes exerted an enhanced gene silencing effect compared to single miRNAs.

Conclusions: Our study provides a comprehensive resource of longitudinal changes in the expression patterns of miRNAs during corticogenesis. Furthermore, we highlight several potential mechanisms through which miRNA regulatory networks can act as modulators of embryonic brain development.

Background

Mammalian brain development is an extraordinarily complex process where neural progenitor cells proliferate and give rise to all neuronal and glial cell types. Numerous transcriptional, post-transcriptional, and epigenetic mechanisms integrate with each other to control progenitor proliferation and self-renewal, differentiation, and lineage commitment as well as migration in a strictly spatio-temporal manner. One of the key regulators of these processes are microRNAs (miRNAs). In most cases, these small RNAs bind to their target mRNAs' 3'- untranslated region (3'UTR) to induce mRNA degradation or translational inhibition. In the canonical pathway, miRNA genes are transcribed into a pri-miRNA in the cell nucleus by PolII/III [1, 2]. In subsequent processing steps, the pri-miRNA is cleaved into a hairpin pre-miRNA by the microprocessor complex Drosha-Dgcr8 and transported to the cytoplasm by Exportin-5 [3-6]. In the cytoplasm, the pre-miRNA is bound and cleaved by a complex containing the RNase Dicer1 to form the mature miRNA duplex [7]. From this duplex, the functional strand is loaded into the RISC complex, guiding it to the 3'UTR's target site [8]. Mice carrying conditional *Dicer* gene deletions in the embryonic telencephalon have shown a variety of phenotypes in the cerebral cortex, such as reduced cell proliferation and impaired neuronal differentiation, increased apoptosis, defective cortical layering and microcephaly [9-14].

In the brain, 70% of all miRNAs are expressed, most of them in a highly cell-type- and developmental-time-specific manner [15]. Given that the total number of human miRNAs is estimated to be ~ 2300, at least 1600 different miRNAs may be expressed in the brain [16]. While this suggests that miRNA regulation is generally important for brain development and function, the specific functions of most miRNAs remain unknown. Single miRNAs are involved in some of these processes including, for example, cell proliferation (e.g. let-7, miR-124, miR-9), neuronal differentiation (e.g. let-7, miR-124, miR-9, miR-128) and migration (e.g. miR-9, miR-124, miR-379-410) [17, 18]. Many of the functionally studied miRNAs are

76 among the most highly expressed in the brain such as miR-9, miR-124 and let-7 [17]. Most
77 miRNAs typically have a relatively weak effect on their target genes [19, 20]. Previous research
78 has suggested that the regulatory potential of a given miRNA could be enhanced by cooperating
79 with other miRNAs in co-targeting networks [21]. This hypothesis is supported by the fact that
80 most 3'UTRs contain more than one miRNA binding site and most miRNAs have matching
81 binding sites in up to several hundred 3'UTRs. A network of miRNAs co-operatively binding
82 at distinct 3'UTR positions can potentially enhance target gene repression by additive or
83 synergistic effects [22, 23]. MiRNA binding at closely spaced binding sites (∼15 – 35 nt) can
84 further enhance the repressive effect [23-25]. We and others have previously identified mRNAs
85 that are targeted by several miRNAs leading to a synergistic or additive repressive effect [19,
86 20, 26]. For example, miRNAs of the miR-379-410 cluster regulate neurogenesis by targeting
87 multiple miRNA binding sites in the N-cadherin 3'UTR in an additive manner [19]. While this
88 highlights the regulatory potential of such miRNA networks during brain development, their
89 detailed composition and temporal dynamics remain poorly characterized. Using an unbiased
90 bioinformatics approach to identify co-targeting networks in mouse tissues, Cherone and
91 colleagues recently found that miRNAs enriched in the human prefrontal cortex had more co-
92 targeting partners than those enriched in other tissues suggesting that miRNA co-targeting is
93 especially important in the brain [20].
94 In the current study, we employed high-throughput small RNA sequencing of the mouse
95 cerebral cortex to create a detailed map of miRNA expression patterns and their longitudinal
96 dynamics at key developmental stages. Using miRNAs whose expression was significantly
97 correlated with developmental time, we constructed a comprehensive co-targeting network in
98 which miRNAs with higher expression levels were associated with significantly more co-
99 targeting relationships. In luciferase assays, we validated the enhanced gene silencing effect of

100 cooperative miRNA binding in a set of target genes involved in the regulation of nervous
101 system development.
102

103 Results

104 *Temporal dynamics of miRNA expression during the cerebral cortex development*

105 To study the expression patterns of miRNAs during mammalian corticogenesis, we performed
106 small RNA sequencing in both female and male mice at a progenitor-dominated developmental
107 phase (embryonic day E14), at an intermediate time point (E17) and at birth (postnatal day P0)
108 when neurons from all six layers of the neocortex have been born [27, 28] (Fig. 1A). Using
109 stringent filtering criteria for expression levels (>10 CPM in at least five samples), we detected
110 a total of 489 miRNAs with only 13 of those corresponding to novel miRNAs. In agreement
111 with previous reports [17, 29], miR-9, members of the let-7 family, miR-128, and miR-124
112 were among the top 20 most abundantly expressed miRNAs in the developing cerebral cortex
113 (Additional file 1, Fig. S1). Principal component analysis (PCA) revealed a distinct separation
114 of samples according to the developmental stage. However E17 and P0 samples had a more
115 similar global expression pattern to each other compared to E14 (Fig. 1B). Since we did not
116 observe apparent differences related to sex, female and male samples were processed together
117 in the subsequent analyses.
118 We detected the highest number of differentially expressed miRNAs in the E14 vs. P0 time
119 points, where 169 miRNAs were up- and 172 were downregulated (Fig. 1C-G). However, the
120 major transcriptional shift already occurred in the transition from E14 to E17, where approx.
121 57% of all detected miRNAs significantly changed their expression level (122 up- and 144
122 down-regulated miRNAs). In contrast, only 36% of all detected miRNAs were differentially
123 expressed in E17 vs. P0 samples (82 up-regulated and 93 down-regulated miRNAs).
124 Interestingly, a higher number of miRNAs were consistently down-regulated at earlier

125 developmental time-points in all pairwise comparisons (45 vs. 32 up-regulated miRNAs, Fig.
126 1C, D, H).
127 To study the expression of miRNAs specifically during neurogenesis, we isolated NPCs from
128 the cortices of mouse embryos at E14 and differentiated them *in vitro* into neurons. Small RNA
129 sequencing of these cells revealed 110 miRNAs that were up-regulated and 113 miRNAs that
130 were down-regulated in NPCs compared to neurons, respectively. miR-124-3p and miR-369-
131 3p were the most significantly up-regulated miRNA in neurons, whereas miR-155-3p and miR-
132 34b-3p were the most significantly up-regulated miRNAs in NPCs (Additional file 1, Fig S2A,
133 D). 66% of the up-regulated (72 out of 110) and 65% of the down-regulated (73 out of 113)
134 miRNAs in NPCs vs. neurons were also differentially expressed in the comparison of bulk
135 samples from E14 vs. P0, confirming the replicability of the expression patterns we observed
136 (Additional file 1, Fig. S2 B-D). Interestingly, these overlapping miRNAs corresponded to
137 43% of all up-regulated and 42% of the down-regulated miRNAs in E14 vs. P0, suggesting
138 that a large proportion of the differentially regulated miRNAs might be attributable to the non-
139 neuronal cells in the bulk samples. This observation is plausible, as gliogenesis takes place
140 roughly between E17 and P0 of cortical development [28, 30] therefore the bulk samples from
141 P0 likely contained both neuronal and non-neuronal cell types.
142

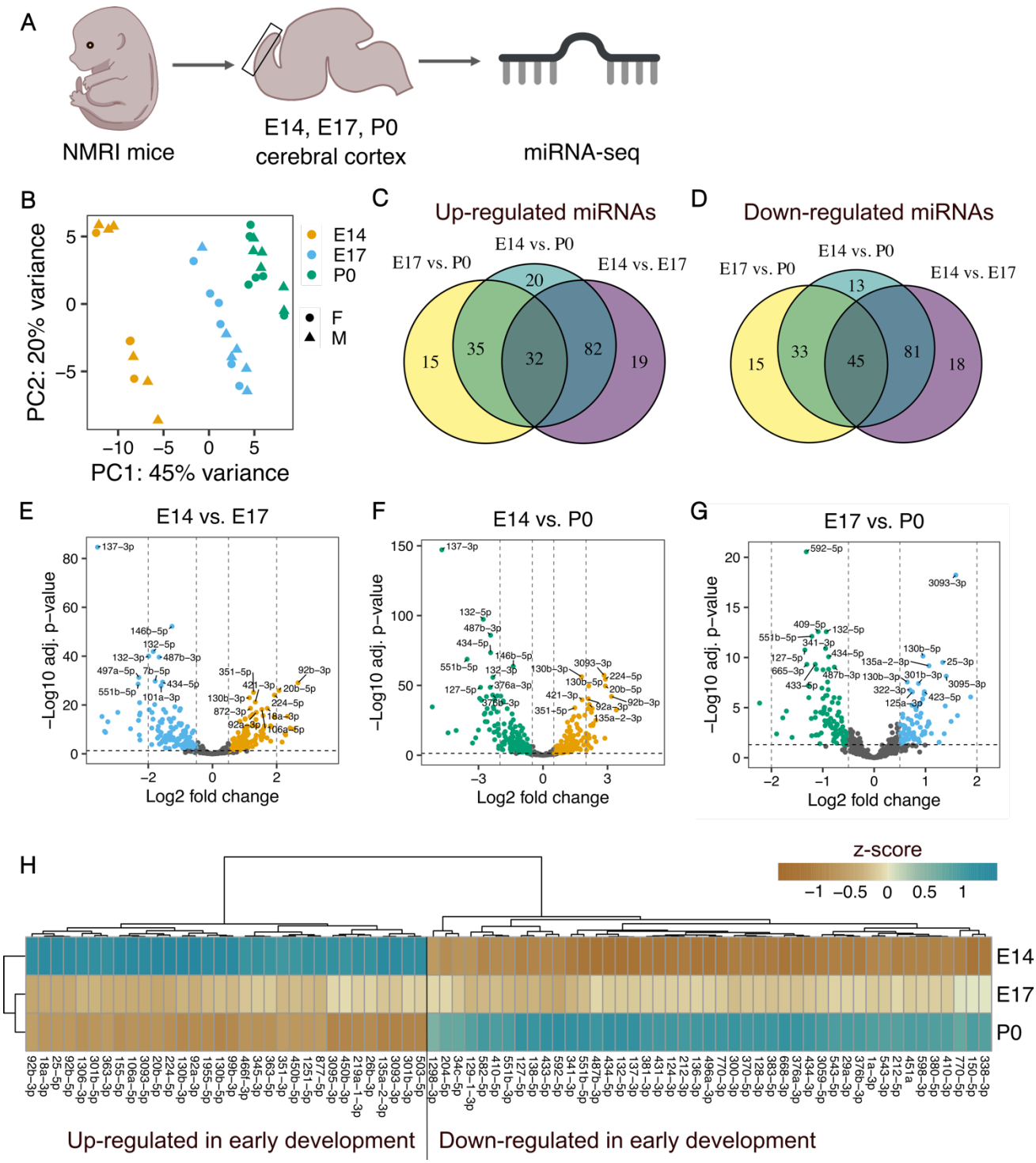

Fig. 1. Expression changes of miRNAs during mouse cerebral cortex development. A Schematic representation of the experimental approach. **B** Principal component analysis of small RNA sequencing samples from the cerebral cortex of female and male mice at different developmental stages. **C** Venn-diagram of up-regulated miRNAs at earlier compared to later developmental stages. **D** Venn-diagram of down-regulated miRNAs at earlier compared to later developmental stages. **E-G** Volcano plots of

149 differentially expressed miRNAs. Positive log2 fold changes indicate miRNAs up-regulated at earlier
150 compared to later developmental stages in each pairwise comparison (E14 vs. E17, E14 vs. P0 and E17
151 vs. P0). **H** Heatmap of miRNAs differentially expressed in each pairwise comparison of different
152 developmental stages. Mean expression values per developmental stage are shown as z-scores.
153

154 ***Weighted co-expression gene network analysis identifies sets of co-regulated miRNAs***
155 ***during the development of the cerebral cortex***

156 Next, we applied weighted co-expression gene network analysis (WCGNA) to construct
157 networks of co-expressed miRNAs and better characterize their transcriptional dynamics along
158 the cortical developmental trajectory. We obtained 18 modules that were assigned to arbitrary
159 colors (Fig. 2A). Module eigengenes (MEs) that correspond to the first dimension in a principal
160 component analysis of the expression matrix of the corresponding WCGNA module, served as
161 proxies for the characteristic transcriptomic signature of each module. Six MEs were
162 significantly negatively correlated with the developmental time point indicating that the
163 miRNAs in the respective modules showed overall reduced expression levels at later compared
164 to earlier developmental stages (Fig. 2B). In contrast, four modules contained miRNAs whose
165 eigengene expression significantly increased during brain development. The black module,
166 which contained the highest number of miRNAs (139), had the strongest negative correlation
167 with the developmental stage. The overall expression pattern captured by the ME, indicated
168 that the black module contained miRNAs whose expression level peaked at E14 and dropped
169 at E17, remaining stable afterwards (Fig. 2C). The green module was the second largest,
170 containing 101 miRNAs with generally linearly increasing expression levels from E14 to P0
171 (Fig. 2D). Remarkably, although these two modules were regulated in opposite directions, they
172 shared most of their targets (6244 common targets, corresponding to 79% of all black module
173 and 72% of all green module targets, Additional file 1, Fig. S3C). Gene ontology analysis using
174 the genes targeted by the miRNAs revealed that both the black and the green modules are

175 involved in the regulation of key nervous system developmental processes such as axon
176 development and guidance, neuron projection, dendrite development, and synapse organization
177 (Fig. 2E, F).

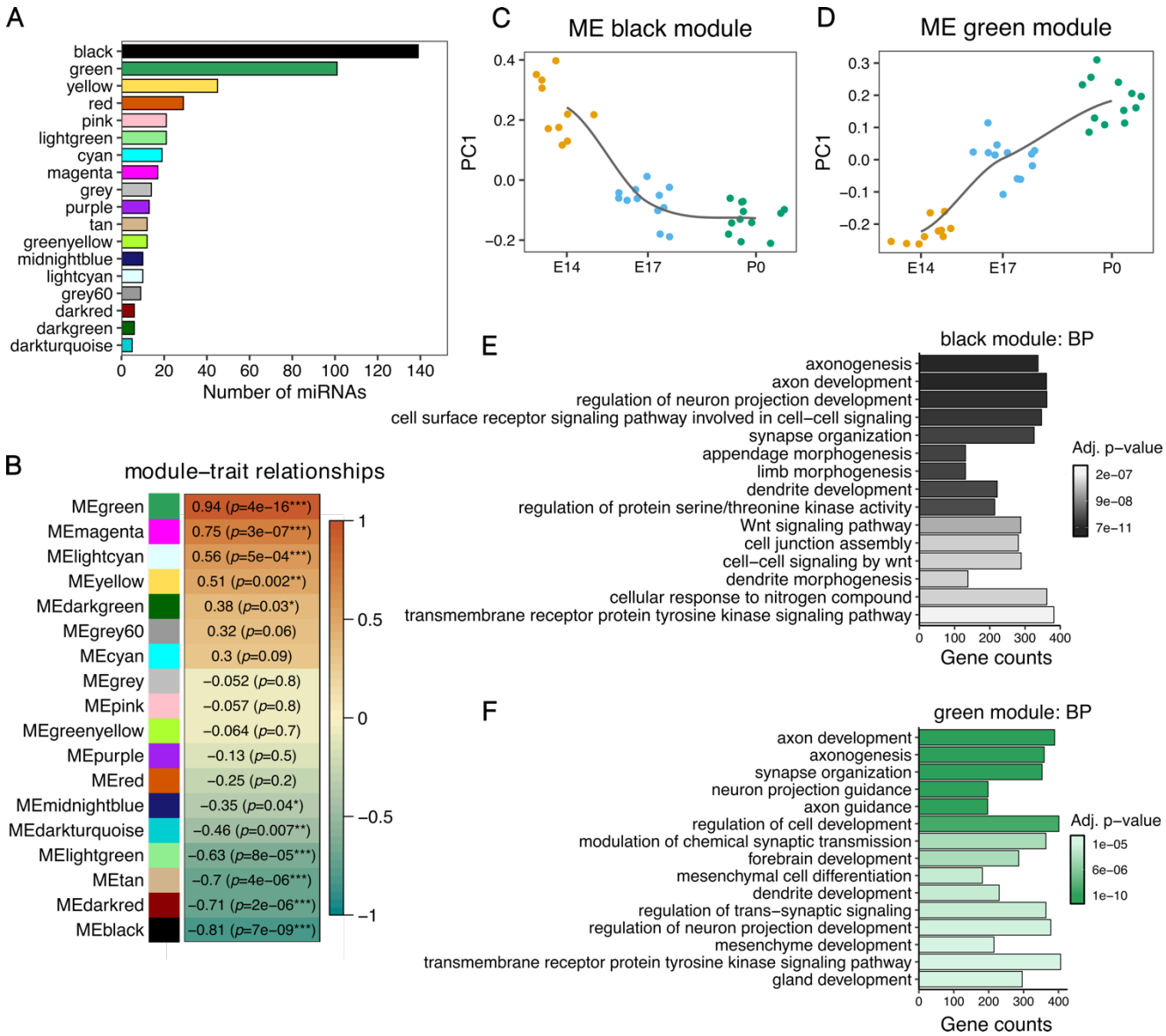

178

179 **Fig. 2 Weighted miRNA co-expression analysis. A** Bar plot showing the number of miRNAs in each
180 co-expression network module. **B** Pearson correlation between developmental stages of the mouse
181 cerebral cortex (E14, E17 and P0) and the module eigengenes (ME). ***p<0.001, ** p<0.01, *p<0.05.
182 **C-D** Module eigengene values at each developmental stage for the black and green module. **E-F** Top
183 15 enriched GO terms for the biological process (BP) category for the gene targets of the black and
184 green modules.

185 To identify key miRNAs at early and late embryonic brain developmental stages, we
186 reconstructed the network structure of miRNAs within the black and green modules and
187 identified key driver (hub) miRNAs as described previously [31, 32]. The black module
188 contained 21 hub miRNAs. 12 miRNAs were also up-regulated in NPCs compared to neurons
189 including members of the miR-92 family - miR-92a, miR-92b (Fig. 3C). Moreover, we
190 detected 18 key driver miRNAs in the green module. Ten of these were also significantly up-
191 regulated in neurons compared to NPCs, including the neuron-specific miR-124 and miR-137
192 (Fig. 3D). This analysis confirmed the stage-specific regulation of a core set of miRNAs during
193 embryonic cortical development.
194 Importantly, all hub miRNAs in the green module and all but one miRNA in the black module
195 were significantly differentially regulated in the E14 compared to the P0 developmental stage
196 (Fig. 3A, B). Furthermore, hub miRNAs in both the black and the green modules showed
197 significantly stronger module membership and gene trait significance estimates compared to
198 the remaining miRNAs in the respective module (Additional File 1, Fig. S3E-H), thereby
199 confirming their importance. Here, module membership corresponds to the correlation between
200 the miRNA's expression and the module eigengene. Furthermore, the gene trait significance
201 represents the correlation between miRNA expression and the trait of interest, in our study –
202 the developmental stage [33].
203 To gain an insight into the relevance of hub miRNAs in regulating target gene expression across
204 development, we re-analyzed RNA-seq data from the mouse cortex at E14.5, E16.5 and P0
205 from the study by Weyn-Vanhentenryck and colleagues [34]. We limited this analysis to the
206 experimentally validated targets of the conserved hub miRNAs that we obtained from
207 miRTarBase [35]. We did not observe a significant deviation in the differential expression of
208 target genes of the black module when comparing P0 and E14.5 (Fig. 3E) which could likely
209 be explained by the overall lower number of validated targets for conserved key driver miRNAs

210 from the black module (Additional File 1, Fig S3D). However, the number of down-regulated
211 targets of the green module's hub miRNAs was significantly higher compared to the overall
212 background distribution of differentially expressed genes (Fig. 3E). The increased proportion
213 of genes with a reduced expression at the time point when the green module's hub miRNAs
214 that target them have their expression peak strongly suggests that these miRNAs are involved
215 in repressing their targets' expression *in vivo*. Interestingly, several important regulators of
216 alternative splicing were among the differentially expressed validated targets (Fig. 3F). Except
217 for *Rbfox2,* all other splice factors were significantly down-regulated at P0 compared to E14.5.
218 Alternative splicing plays a pivotal role in neuronal differentiation [36], axonogenesis [37] and
219 synapse formation [38]. Our findings suggest that mediating the expression of crucial splice
220 factors is another mechanism through which miRNAs might be involved in shaping brain
221 development. In line with this, the green module hub miR-124-3p is known to repress *Ptbp1*
222 expression and thereby induce neuron-specific alternative splicing programs required for
223 neuronal differentiation [39].

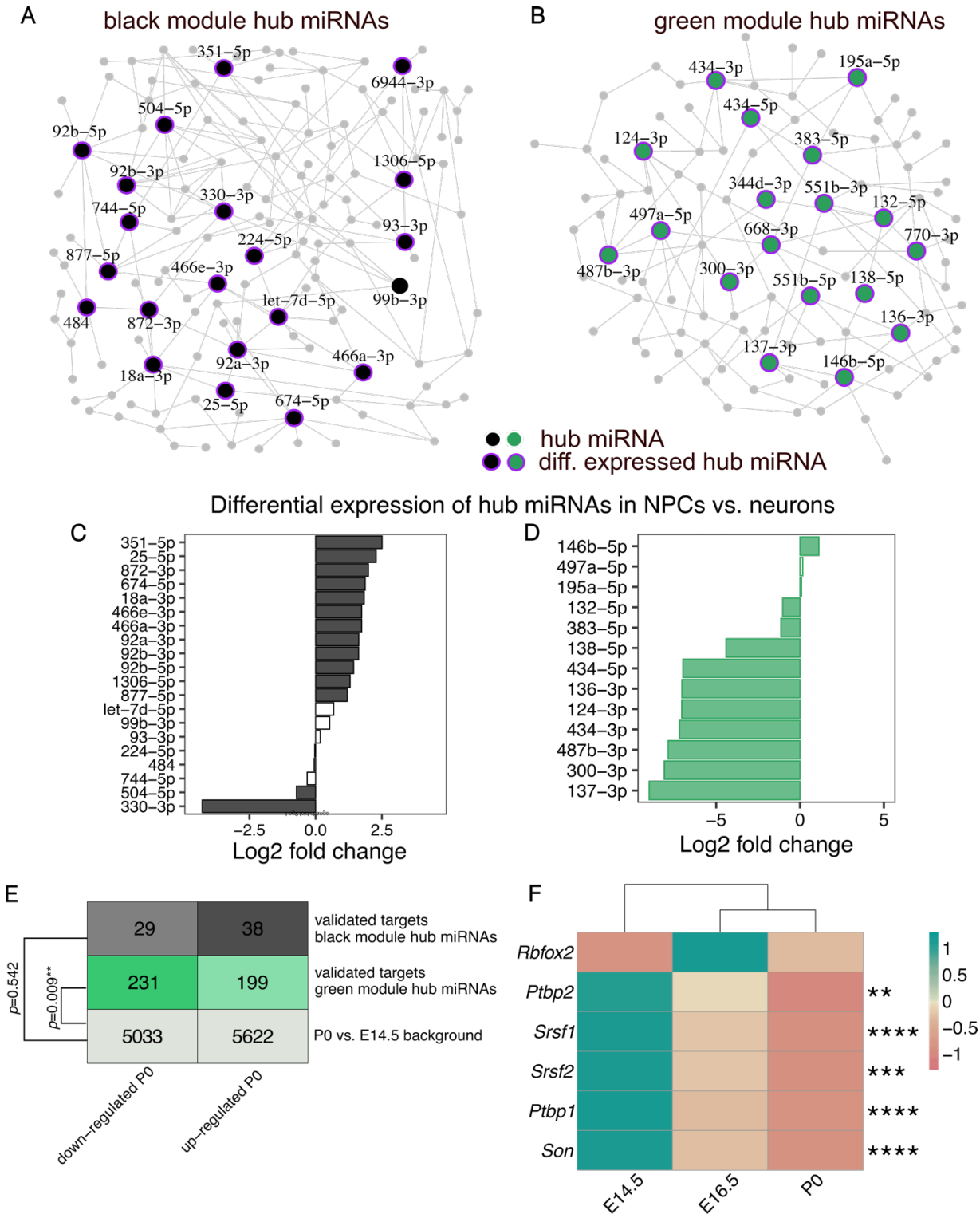

Fig. 3 Hub miRNAs in the black and green modules. Network plot showing the hub miRNAs in the black **(A)** and green **(B)** modules. Hub miRNAs are represented as bigger nodes. Purple halos around the nodes indicate miRNAs that are significantly differentially expressed between E14 and P0. **C-D** Differential expression of hub miRNAs from the black **(C)** and green **(D)** module detected in the NPCs versus neurons analysis. Positive log2 gold changes indicate an up-regulation in NPCs, negative values

230 correspond to up-regulation in neurons. White bars indicate non-significant fold changes. **E** Distribution
231 of differentially expressed genes between E14.5 and P0. The overall number of genes as well as the
232 number of these genes that are validated targets from miRNAs in the black and green module as
233 obtained from miRTarBase are given. The comparison of the distribution of differentially expressed
234 targets of the black or green module from the overall distribution of differentially expressed genes was
235 performed with a Fisher's exact test. **F** Z-score transformed average expression of splicing factors that
236 are validated targets of miRNAs from the green module at E14.5, E16.5 and P0. Asterisks denote the
237 significant differential expression of the respective gene at P0 compared to E14.5. ** $p<0.01$, ***
238 $p<0.001$, **** $p<0.0001$. The expression values in E and F were obtained from the study by Weyn-
239 Vanhentenryck et al. [34].
240
241 ***Prediction of miRNA co-targeting networks in the developing cerebral cortex***
242 WCGNA revealed that clusters containing multiple miRNAs are co-expressed during cortical
243 development. Furthermore, when looking at the predicted targets of the black and green
244 modules, we observed that only approx. 30% were potentially targeted merely by a single
245 miRNA. On average, each gene was associated with more than 3 miRNAs (Additional file 1,
246 Fig. S3A-B). This apparent redundancy of simultaneously expressed miRNAs that putatively
247 bind to overlapping sets of genes supports the previously proposed hypothesis that miRNAs
248 might act together to co-operatively exert stronger gene silencing. To construct a
249 comprehensive co-targeting network of miRNAs in the developing cerebral cortex, we
250 designed a statistical framework that allowed us to detect which miRNAs share significantly
251 more targets than expected by chance. In this analysis, we included all miRNAs whose module
252 eigengene was correlated significantly with developmental time in the WCGNA (Fig. 2B).
253 Furthermore, we only considered conserved miRNAs with at least 300 conserved targets and
254 distinct seed sequences [20]. miRNAs belonging to the same broad conserved family and
255 thereby having identical seed sequences, were grouped together for the statistical testing. After

256 applying these filtering criteria, we performed the co-targeting prediction with a set of 77
257 miRNA families corresponding to 106 individual miRNAs (Fig. 4A). We detected 1216
258 significant co-targeting pairs with an adjusted p-value <0.05 (Figure 5) and each miRNA had
259 on average 41 co-targeting relationships (Fig. 4B). Interestingly, the number of significant co-
260 targeting relationships was positively correlated with the miRNA's average expression level
261 (Fig 4C). This finding implies that important miRNAs might need to be produced at higher
262 amounts to facilitate their involvement in multiple cooperative gene silencing interactions in
263 the co-targeting network. Importantly, hub miRNAs such as mir-92a/b from the black module
264 as well as miR-124 and miR-137 from the green module were among the miRNAs with the
265 highest expression level and highest number of co-targeting relationships (Fig. 4C) indicating
266 that these miRNAs might be master regulators in both co-expression and multi-targeting
267 networks. As expected, the length of the 3' UTR was positively correlated with the number of
268 significant miRNA pairs targeting a gene (Fig. 4D). Interestingly, *Nova1*, was among the top
269 10 genes involved in the highest number of co-targeting associations. NOVA1 is a neuron-
270 specific splice factor that is crucial for neuronal viability [40] and regulates the alternative
271 splicing of genes involved in synapse formation [41]. In line with this, we detected a significant
272 *Nova1* expression increase in cortical samples at P0 compared to E14.5 (log2 fold change =
273 0.84, adj. p-value <0.0001) when re-analyzing the RNA-seq data from Weyn-Vanhentenryck
274 et al. [34]. Thus, our findings further highlight the potential importance of miRNAs in
275 regulating neurodevelopment by influencing the expression of crucial effectors of alternative
276 splicing processes.
277 Remarkably, we detected the strongest co-targeting relationship between miR-137 and the
278 miR-25/miR-363/miR-92 family, sharing 353 common gene targets (Fig 4F). While miR-137
279 was up-regulated at later developmental stages, all members of the miR-25/miR-363/miR-92
280 cluster were regulated in the opposite direction. This prominent association between hub

281 miRNAs, that were not co-expressed, prompted us to investigate the distribution of intra-
282 modular (between miRNAs from the same module) and inter-modular (miRNAs from different
283 modules) co-targeting relationships for the black and green WCGNA modules. While we
284 expected that relationships between co-expressed miRNAs might be enriched, we indeed
285 observed a comparable distribution of intra- and inter-modular co-targeting pairs (Fig. 4E).
286 These findings point to two distinct potential regulatory mechanisms justifying the need for
287 miRNAs to share significantly more targets than expected by chance. On the one hand,
288 miRNAs with common targets regulated in opposite directions during cortical development
289 might arise from the need to facilitate target gene regulation at different time points or in
290 distinct cell types. On the other hand, co-expressed miRNAs that regulate the same genes could
291 cooperatively bind to their targets to exert a stronger repressive effect compared to single
292 miRNAs.
293

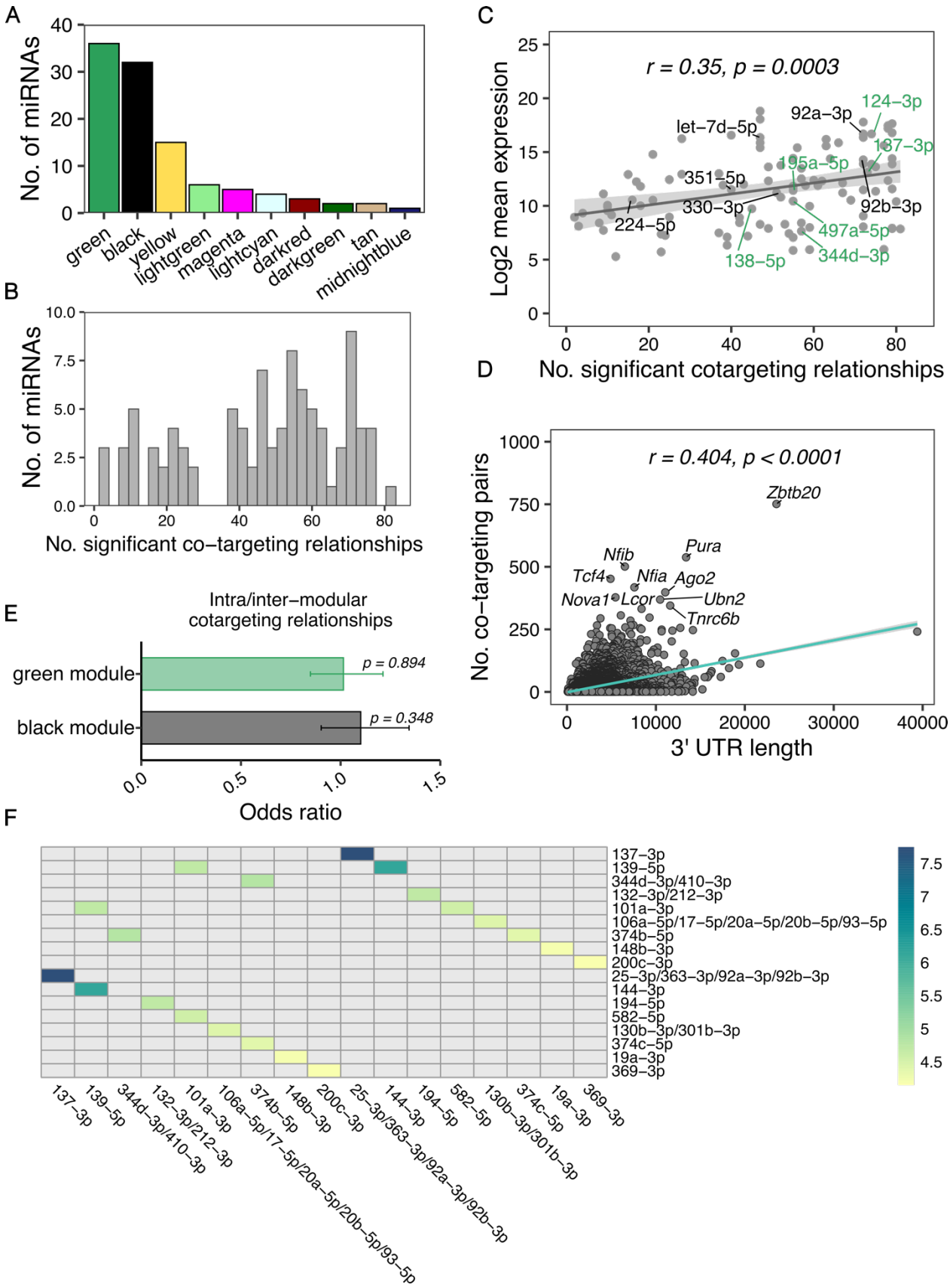

Fig 4. Features of the miRNA co-targeting network of the developing cerebral cortex. A Bar plot showing the number of miRNAs from each module that were included in the co-targeting analysis after

297 applying the filtering criteria. **B** Histogram of the number of miRNAs having a specific number of
298 significant co-targeting relationships. **C** Scatter plot indicating the correlation between the number of
299 co-targeting relationships with the log2-transformed miRNA's average expression level; *r* corresponds
300 to Pearson's correlation coefficient. Labels indicate hub miRNAs from the WCGNA analysis of the
301 black and green modules **D** Correlation between the 3' UTR length of target genes and the number of
302 significant co-targeting miRNA pairs the genes are targeted by; *r* corresponds to Pearson's correlation
303 coefficient. **E** Bar plot with the association of the number of intra-modular (between miRNAs of the
304 same module) and inter-modular (involving miRNAs from different modules) co-targeting
305 relationships. Odds ratios were obtained with a Fisher's exact test. Error bars indicate the 95%
306 confidence interval. **F** Heatmap with the top 10 strongest co-targeting relationships between pairs of
307 miRNAs/conserved miRNA families. Values indicate odds ratios as measures of association between
308 the co-targeting pairs.
309

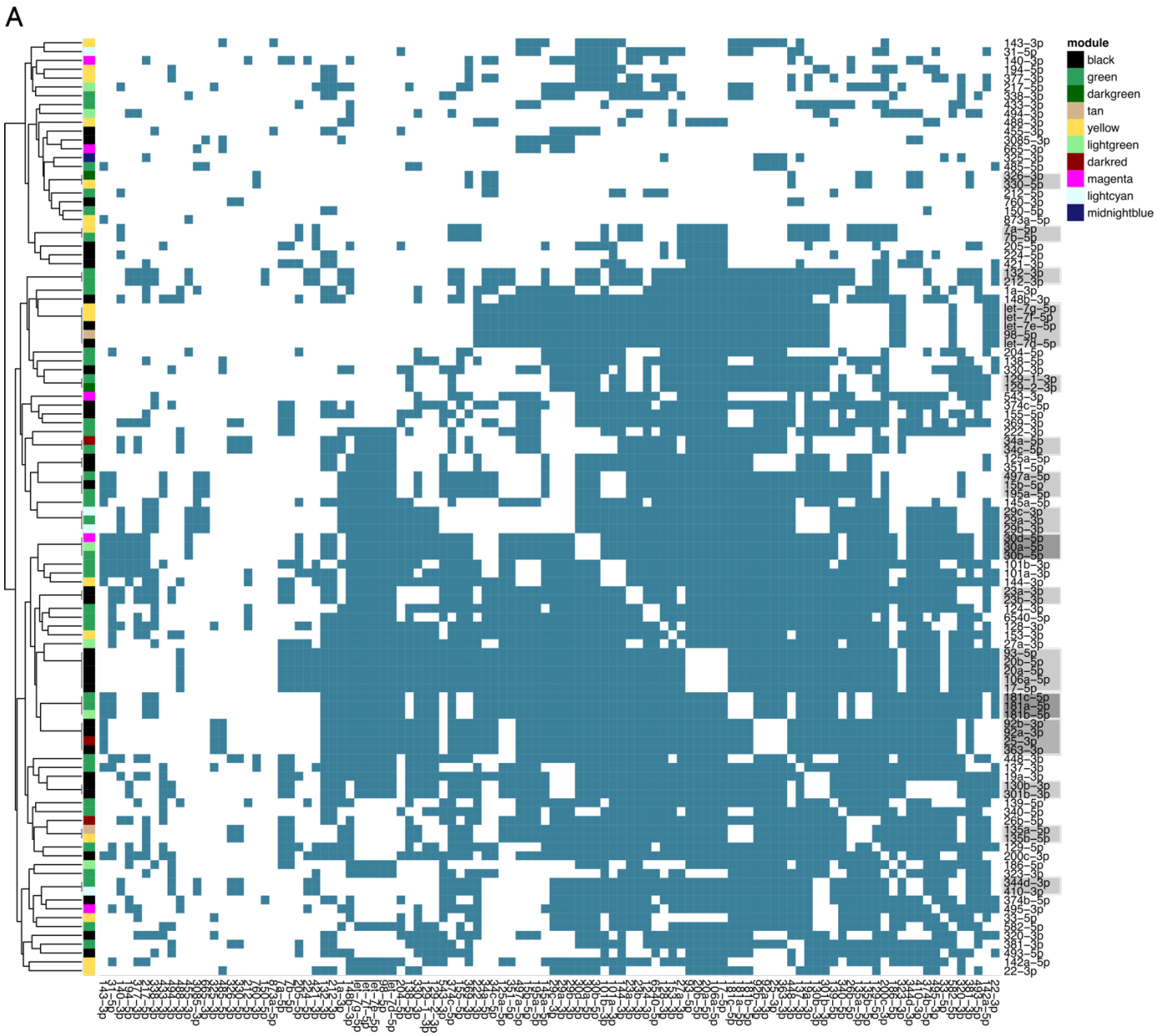

Fig.5 Significant co-targeting miRNA pairs. Colored squares on the heatmap indicate significant co-targeting relationships. miRNAs that belong to the same conserved family and therefore have identical co-targeting relationships to each other, are indicated with gray rectangles on the vertical axis of the heatmap.

Enhanced gene silencing effect by cooperative binding of co-expressed miRNAs

To validate the hypothesis that co-expressed miRNAs bind co-operatively to their common targets to enhance their repressive effect, we employed luciferase reporter assays focusing on

319 miRNAs that were up-regulated during embryonic brain development. We performed a gene
320 ontology term look-up of all targets and filtered potential candidate genes for terms including
321 brain/forebrain development and (central) nervous system development. Then we looked for
322 genes with two or more conserved binding sites in their 3' UTR for miRNAs up-regulated
323 during cortical development. Using this strategy, we compiled a list of 7 candidate target genes
324 (*Neurod1, Apc, Dcx, Ndst1, Zeb2, Src* and *Cxcl12*) and 5 miRNAs (miR-128-3p, miR-129-5p,
325 miR-135b-5p, miR-137-3p and miR-153-3p).
326 First, we performed RT-qPCR analyses to validate the expression patterns that we observed in
327 the bulk sequencing of the miRNAs selected for luciferase assays. All 5 miRNAs showed
328 significantly increased expression levels in neurons compared to NPCs with mean relative
329 quantification (RQ) values ranging from 2.9 to 3987 in the case of miR-135b-5p (Additional
330 file 1, Fig. S4 A-E). Furthermore, all miRNAs were associated with increased expression at
331 later developmental stages in cortical tissue samples. The relative expression of miR-128-3p
332 and miR-135b-5p significantly increased over all time points analyzed (Additional file 1, Fig.
333 S4 F, H). miR-137-3p and miR-153-3p were associated with a significantly higher expression
334 levels at E17 and P0 compared to E14 (Additional file 1, Fig S4 I, J). miR-129-5p was the only
335 miRNA that showed a non-significant trend of higher expression at later developmental stages
336 (Additional file 1, Fig. S4 G).
337 Subsequently, for each luciferase reporter assay, we cloned the target gene's 3'UTR fragment
338 containing the binding sites of the selected miRNAs, downstream of the synthetic *Renilla*
339 luciferase gene into the psiCHECK^{TM}-2 vector, which also expresses firefly luciferase as
340 internal control. Plasmids were then co-transfected into HEK293 cells with different
341 combinations of miRNA mimics and luciferase activity was evaluated in cell lysates 48 h later.
342 The fold change of *Renilla*/firefly luciferase signal was normalized to a control group

343 containing either a non-targeting siRNA or a miRNA mimic without a predicted binding site
344 in the 3'UTR fragment of the target gene.
345 The first gene we investigated, *Neurod1*, is an important transcription factor regulating
346 neuronal differentiation and migration in the developing cerebral cortex [42]. *Neurod1* contains
347 binding sites for miR-137-3p and miR-153-3p that were previously demonstrated to co-
348 operatively repress the gene's expression [20]. Therefore, we used this experiment as a positive
349 control. We independently cloned two *Neurod1* 3' UTR fragments with different lengths (274
350 bp and 1188 bp, respectively). The luciferase activity was significantly reduced in cells
351 transfected with the combination of miR-137-3p and miR-153-3p compared to individual
352 miRNAs as well as two different negative controls (siRNA and miR-128-3p), thereby
353 confirming the co-targeting effect previously observed (Fig. 6A-B).
354 *Src*, a proto-oncogene that codes for a non-receptor protein tyrosine kinase is another important
355 neurodevelopmental regulator that contains binding sites for both miR-137-3p and miR-153-3p in
356 its 3'UTR. *Src* is expressed at steadily high levels in the mouse neocortex from E12.5 to P1 and
357 overexpression of this gene leads to impaired neuronal migration due to altered adhesion properties
358 and cytoskeletal dynamics [43]. We observed that the combination of both miRNAs exerted a
359 significantly stronger repressive effect on *Src* compared to each individual miRNA (Fig. 6C).
360 As an additional target gene for the reporter assays, we selected *Cxcl12* which is also an important
361 regulator of early brain development. *Cxcl12* is involved in migration of NPCs, early localization
362 of Cajal-Retzius cells in the developing cortex, and in axon guidance and pathfinding [44, 45].
363 *Cxcl12* is a predicted target of miR-137-3p and miR-135b-5p. Luciferase reporter assays showed
364 that co-transfection with both miRNAs significantly increased the repressive effect compared to
365 the negative siRNA control and treatment with each miRNA separately (Fig. 6D).
366

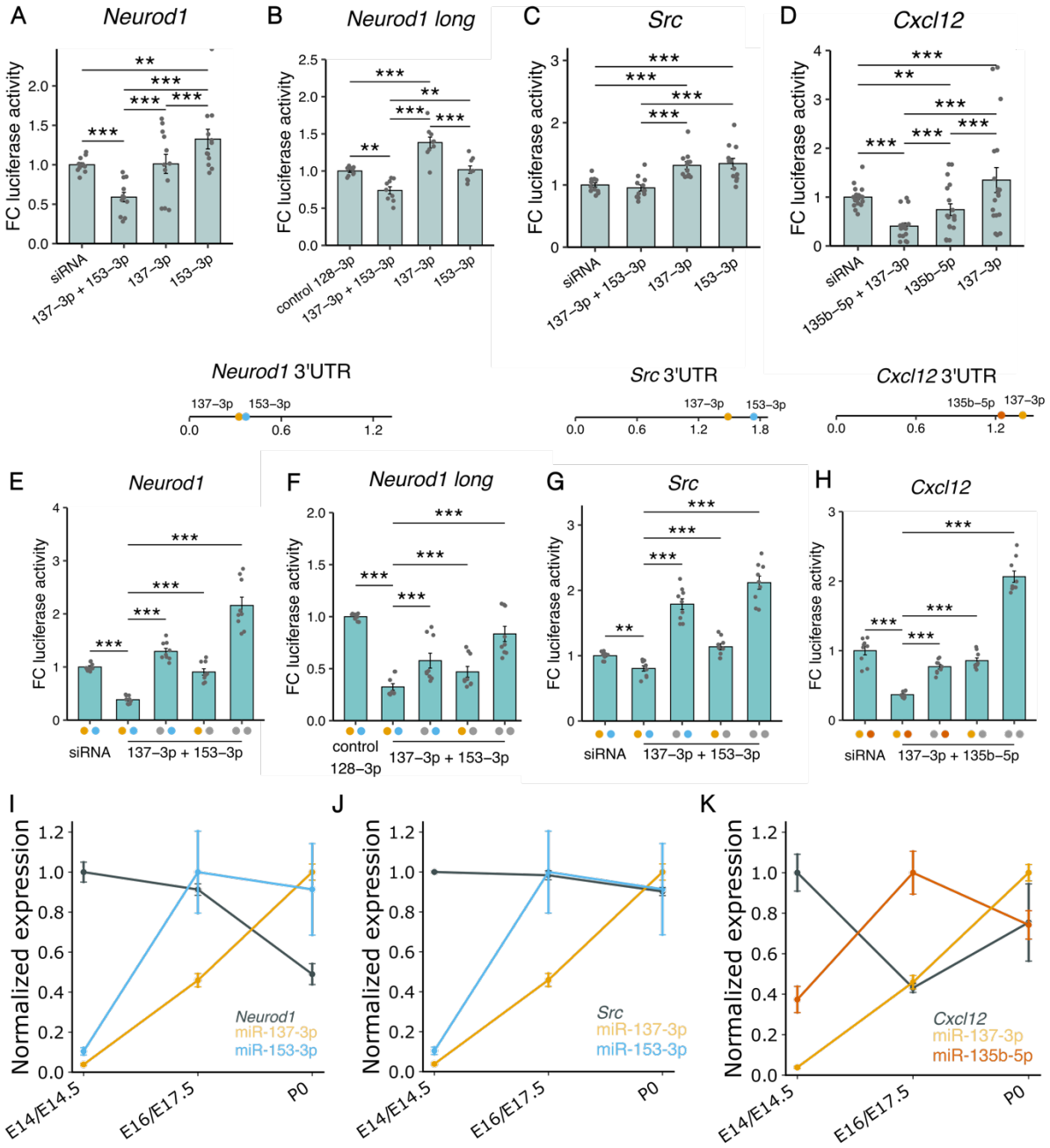

Fig. 6 Luciferase activity in lysates of HEK293 cells transfected with plasmids containing 3' UTR fragments of target genes. A-D Lysates were co-transfected with different combinations of miRNA mimics. Fold change (FC) of luciferase activity was obtained by calculating the ratio of *Renilla* luciferase and firefly luciferase activity and then normalizing to the mean of the control siRNA or miRNA group. Locations of the binding sites in the 3' UTR of the respective gene are represented by colored dots. The length of the 3' UTRs is indicated in kbp. **E-H** Fold change of luciferase activity was measured after introducing point mutations in the binding sites of the miRNAs in the 3' UTR regions. Colored dots on the x-axis indicate that the binding site of the respective miRNA was intact, gray dots indicate a mutated binding site. **I-K** Expression of miRNAs and target genes during

embryonic brain development. Expression values were normalized to a 0-1 range. Target gene expression values were measured at E14.5, E16.5 and P0 and were obtained from the study by Weyn-Vanhentenryck et al.[34]. Data are shown as mean ± standard error of the mean and individual values. *p<0.05, ** p<0.01, *** p<0.001, two-way analysis of variance followed by Tukey's post-hoc test.

In contrast, we did not observe a significant co-targeting effect for miR-153-3p with miR-129-5p and miR-137-3p with miR-128-3p in reporter assays with *Apc* and *Ndst1,* respectively (Additional file 1, Fig S5A, C). Furthermore, we aimed to investigate if higher-order co-targeting interactions, including three miRNAs would exert stronger silencing effects on gene expression. To this end, we co-transfected cells with plasmids containing the 3' UTR fragment of the *Dcx* gene and mimics of miR-128-3p, miR-129-5p, and miR-135b-5p (Additional file 1, Fig S5B). In an additional assay, we cloned the 3' UTR of *Zeb2* and co-transfected cells with its targeting miRNAs – miR-129-5p, miR-137-3p and miR-153-3p (Additional file 1, Fig S5D). Treatment with different miRNA mimics significantly reduced luciferase activity compared to the siRNA control in the *Zeb2* assays. However, we did not observe a significant cooperative repressive effect for either *Dcx* or *Zeb2.*

To confirm that the cooperative silencing effect for *Neurod1, Src,* and *Cxcl12* was mediated via direct binding of the miRNAs, we employed *in vitro* site-directed mutagenesis to introduce mutations in the miRNA binding sites of the 3' UTRs. We generated plasmids carrying a mutation in one of the binding sites or in both binding sites of the respective co-targeting pair. For all three genes, we observed the highest luciferase activity in the cell lysates where both miRNA binding sites were mutated. Conversely, the strongest repressive effect was detected when both binding sites were intact, thereby confirming that miRNAs acted co-operatively to exert stronger gene silencing (Fig. 6E-H). Furthermore, we investigated the expression patterns of these three genes by employing the data from Weyn-Vanhentenryck et al. [34]. *Neurod1* was significantly down-regulated at P0 compared to E14.5 and E16.5, correlating negatively

402 with the expression pattern of the co-targeting pair mir-137-3p and miR-153-3p (Fig. 6I,
403 Additional file 1, Fig S6A). While *Src* was not differentially regulated, it still had its expression
404 minimum at P0 (Fig. 6J, Additional file 1, Fig. S6B). Interestingly, *Cxcl12* had a significantly
405 reduced expression only at E16.5 compared to E14.5, but this pattern negatively correlated
406 with the expression peak of miR-135b-5p at E17 (Fig. 6K, Additional file 1, Fig. S6C). These
407 matching *in vivo* expression patterns of the miRNAs and the genes they co-target lend further
408 support to the biological relevance of the co-operative miRNA gene silencing we observed in
409 the luciferase assays.
410

411 **Discussion**

412 Our study provides a detailed map of the longitudinal changes in miRNA expression patterns
413 that occur in the transition between NPCs and neurons as well as *in vivo* at key stages of
414 embryonic cortical development in the mouse. Previous studies employing high-throughput
415 sequencing to examine miRNA composition in the embryonic cortex have focused on a single
416 time point [29, 46]. In contrast, *in situ* hybridization-based technologies have successfully
417 profiled miRNA expression in different embryonic brain structures and at multiple time points
418 [47], however, this analysis has been limited to a pre-selected set of miRNAs. To our
419 knowledge, this is the first high-throughput longitudinal investigation, therefore providing a
420 valuable resource for elucidating the regulatory role miRNAs play during embryonic
421 corticogenesis.
422 Remarkably, the majority of the miRNAs significantly altered their expression level already at
423 the transition from E14 to E17. This predominantly neurogenic phase is characterized by a
424 complex interplay of multiple processes that shape late-stage embryonic corticogenesis [48].
425 At E14, radial glia cells in the ventricular zone have switched from symmetrical to
426 asymmetrical divisions to give rise to the basal progenitors that later generate neurons.

427 Subsequently, newly born neurons migrate out of the ventricular zone to the upper layers of
428 the neocortex where they differentiate into mature neurons. Upon neurogenesis completion at
429 around E17, neural stem cells give rise to the other brain cell types including astrocytes and
430 oligodendrocytes [28, 30]. Cell fate commitment and neuronal identity are determined by
431 specialized transcriptional programs that occur in sequential waves and eventually result in the
432 immense cell type diversity observed in the brain [49, 50]. The dynamic changes of miRNA
433 expression we detected indicate that miRNA networks can act as quick regulators of these
434 transcriptional programs by controlling the expression of cell-type specific genes [51].
435 miRNA-mediated transcriptional inhibition could also contribute to reducing excess levels of
436 target mRNA arising as noise from transcriptional bursts and thereby ensuring appropriate cell-
437 type or developmental-stage specific expression. In line with this, we observed an enrichment
438 of down-regulated genes at P0 compared to E14, which were validated targets of hub miRNAs
439 in the green module (Figure 3E). Interestingly, several proliferative genes [50], including *Sox2,*
440 *Notch3, Sp8,* and *Ccna2* were among the significantly down-regulated validated green module
441 hub miRNA targets, which supports the hypothesis that miRNAs contribute to regulating the
442 transcriptional programs that determine cell identity. For instance, the canonical NPC marker
443 *Sox2* is a crucial regulator of the maintenance and self-renewal of progenitors [52, 53], and
444 blocking its expression promotes neuronal differentiation [52]. In fact, a recent review
445 highlighted a complex regulatory interplay between SOX transcription factors and miRNAs
446 that guide distinct cellular activities in the developing and adult brain under physiological and
447 pathological conditions [54].
448 By employing a co-expression network analysis, we detected sets of co-regulated miRNAs
449 with individual miRNAs acting as hubs at early (e.g., miR-92a/b) and late (e.g., miR-124 and
450 miR-137) stages of neurogenesis. miR-92 is a part of the miR-17-92 cluster that is involved in
451 the maintenance of neural stem cells, and its genetic ablation results in a reduced pool of neural

452 stem and radial glia cells and a premature transition to intermediate progenitors [55].
453 Furthermore, miR-137 has been reported previously to influence neuronal differentiation via a
454 regulatory loop between TLX and miR-137' downstream target LSD1 [56].
455 Another crucial mechanism through which miRNAs can influence the development of the
456 cerebral cortex is via the regulation of RNA-binding proteins. In line with this, we observed
457 that several effectors of alternative splicing whose expression significantly changed during
458 embryonic corticogenesis were validated targets of hub miRNAs in our analysis (Figure 3F).
459 In this context, miR-124 represents one of the most well-studied examples in neuronal
460 differentiation. miR-124 targets PTBP1, a protein that represses neuronal splice patterns. The
461 upregulation of miR-124 in neurons is sufficient to suppress the expression of *Ptbp1* and
462 thereby induce the necessary splicing changes for the transition from NPCs to neurons [39].
463 Thus, miRNAs could act as a post-transcriptional mechanism ensuring the precise spatio-
464 temporal expression of RNA-binding proteins which is critical for proper development of the
465 central nervous system [57].
466 Surprisingly, the gene silencing effect of most miRNAs is modest despite their crucial
467 regulatory potential [58], indicating that – with the exception of hub miRNAs – they might be
468 fine tuners rather than master regulators of embryonic brain development. However, the
469 redundancy of multiple co-expressed miRNAs sharing the same target genes supports the
470 mechanism of co-operative binding to enhance the gene-silencing effect of individual miRNAs
471 [20]. Accordingly, we confirmed the co-targeting for several neurodevelopmentally relevant
472 genes in luciferase assays (Figure 6). Furthermore, the negative correlation between the *in vivo*
473 miRNA and target expression peaks strongly suggests that co-targeting is a biological
474 phenomenon that can occur during embryonic cortical development. As 3' UTRs of mRNAs
475 expressed in the brain are longer compared to other tissues [59] and this length even increases

476 in neuronal transcripts [60], the brain indeed offers extremely favorable conditions for the
477 emergence of miRNA multi-targeting networks [20].
478 Notably, significant co-targeting relationships between co-expressed miRNAs were as likely
479 as co-targeting associations between miRNAs regulated in opposite directions. Apart from
480 simultaneous cooperative biding to enhance gene silencing, this observation points to an
481 alternative evolutionary need for the presence of multiple binding sites for distinct miRNAs in
482 the same gene, namely regulating the expression at different time points or in diverse cell types.
483 Accordingly, Nowakowski and colleagues recently reported cell-type specific miRNA-mRNA
484 interactions in the developing human cortex using a single-cell profiling strategy [51]. Thus,
485 distinct miRNAs might be responsible for silencing temporally or spatially abnormal
486 expression of an overlapping set of genes. This explains our observation of miRNAs with
487 opposite expression patterns that share more targets than expected by chance.
488

489 **Conclusions**

490 In summary, we detected dynamic changes in miRNA expression during embryonic brain
491 development with distinct miRNAs acting as hubs in co-expression and co-targeting networks.
492 Furthermore, we identified modulation of transcriptional programs and expression levels of
493 RNA binding proteins as important potential regulatory mechanisms of miRNA networks that
494 could influence corticogenesis. Our study also provides additional evidence that simultaneous
495 binding to common targets increases the transcriptional repression effect of miRNAs. To
496 further resolve the complexity of mRNA-miRNA as well as miRNA co-targeting networks in
497 distinct cell types *in vivo,* future studies should focus on single-cell high-throughput profiling
498 techniques.
499

500 **Methods**

501 **miRNA sequencing of the developing mouse cerebral cortex and in NPCs/neurons**

502 For NPC/neuron culture, the cortices of E14.5 NMRI embryos (Janvier Labs; Le Genest-Saint-
503 Isle, France) were dissected and collected in cooled DMEM high glucose media (Gibco Life
504 Technologies) and processed into single cells by trypsin digestion. For NPC and neuron
505 culture, 0.2x10^6 cells per well and 1.4x10^6 cells per well, respectively, were seeded on Poly-
506 L-ornithin and Laminin coated 6 well plates. The NPCs were cultured in neurobasal medium
507 containing 2% B27 -VitA supplement (Gibco Life Technologies), 500µM Glutamax (Gibco
508 Life Technologies) and EGF (10ng/ml) and FGF (10ng/ml). For neural differentiation, the cells
509 were cultured in neurobasal medium containing 2% B27 supplement (Gibco Life
510 Technologies) and 500 µM Glutamax (Gibco Life Technologies). Total RNA, including
511 miRNA, was isolated from the NPCs and neurons as well as from cortices of female and male
512 NMRI embryos (Janvier Labs; Le Genest-Saint-Isle, France) at the time points E14, E17 and
513 P0 (n=6 embryos per sex and time point) using the Qiagen miRNeasy mini kit (CatNo. 217004;
514 Qiagen; Hilden, Germany). 500 ng of total RNA, including miRNA, were used as an input for
515 library preparation with the Bioo Scientific NextFlex small RNA v3 Seq Kit (CatNo. NOVA-
516 5132-05; Bioo Scientific; Austin, USA). Library preparation was conducted according to the
517 kit manual. Size distribution and concentrations of the prepared libraries were checked by
518 Qubit dsDNA High Sensitivity Assay (CatNo. Q32851; Thermo Scientific; Waltham, USA).
519 0.5 nanomoles (NPCs/neurons) or 4 nanomoles (Cortex samples) of the prepared miRNA
520 libraries were loaded on a High Output v2 kit (75 cycles) Illumina cartridge which was run on
521 a NextSeq 500 device.

522

523 **miRNA sequencing data pre-processing**

524 After the sequencing, bcl2fastq v2.17.1.14 conversion software (Illumina, Inc.) was used to
525 demultiplex sequencing data and convert base call (BCL) files into fastq files. The trimming

526 of the fastq files was conducted in two steps as suggested by the NEXTflex™ Small RNA
527 Trimming Instructions. Briefly, sequencing adapters (TGGAATTCTCGGGTGCCAAGG)
528 were trimmed and reads shorter than 15 nucleotides were removed from further analysis.
529 Afterwards, 4 bases from either side of each read were trimmed using Cutadapt v1.18. Quality
530 control checks were performed on the trimmed data with FastQC v0.11.7.
531
532 **miNRA differential expression analysis**
533 miRNA samples with at least 20 million reads were further analyzed. Using miRDeep's
534 v2.0.1.2 *mapper.pl* script, miRNA reads were mapped to the *Mus musculus* GRCm38 genome.
535 Afterwards, known and novel miRNA were identified using the *miRDeep2.pl* script. Prior to
536 differential expression analysis, miRNAs with CPM expression values less than 10 were
537 filtered out using edgeR v3.30.3. Differential expression analysis was then performed with
538 DESeq2 v1.28.1. miRNAs with an adjusted p-value <0.05 and an absolute log fold change
539 exceeding 0.5 were considered differentially expressed. P-values were corrected for multiple
540 comparisons with the Benjamini-Hochberg method.
541
542 **Weighted gene co-expression network analysis**
543 We performed a Weighted Correlation Network Analysis (WGCNA) [33] to find clusters or
544 "modules" of co-expressed miRNAs. For the analysis, a *bicor* correlation type and a *signed*
545 network type with soft-thresholding power of 24, minimal module size of 5 and dynamic tree
546 cut height of 0.2 were applied. Target prediction of the miRNAs in each module was performed
547 using the TargetScanMouse database v7.2 [61]. Functional enrichment analysis of the different
548 modules in the co-expression network was conducted using the clusterProfiler v4.6.2 R
549 package and the target genes of the miRNAs in the respective module as input.
550

551 **Key driver analysis**

552 To identify hub (or key driver) miRNAs in the modules of the co-expression network, we
553 performed a key driver analysis as previously described [31, 32]. First, we used the algorithm
554 for the reconstruction of cellular networks (ARACNE) [62] as implemented in the bnlearn R
555 package v4.8.3 to obtain an undirected gene regulatory network from the expression levels of
556 the miRNAs in the respective WGCNA module. Next, we performed key driver analysis on
557 the ARACNE reconstructed network using the KDA R package v0.2.2
558 (https://github.com/mw201608/mnml-public/tree/master/pkgs) to identify important
559 regulatory miRNAs.

560

561 **Analysis of publicly available RNA-seq data of the developing mouse cortex**

562 To explore the expression of target genes during cortical development, we re-analyzed publicly
563 available data from the study by Weyn-Vanhentenryck et al.[34] containing RNA-seq of the
564 mouse cortex. We focused on E14.5, E16.5, P0 as these were comparable with the time points
565 in our study. Fastq files were downloaded from the NCBI Short Read Archive, accession
566 number SRP055008. After trimming with BBDuk v39.01, reads were mapped to the Gencode
567 mm39 reference genome (released 19.10.2022) using STAR v2.7.10b. A count matrix was
568 obtained using FeatureCounts provided by SubRead v2.0.6. Differential expression analysis
569 was performed with DESeq2 v1.40.1 with default settings. Genes with an adjusted p-value
570 (Benjamini-Hochberg method) < 0.05 were considered to be differentially expressed.

571

572 **miRNA expression profiling using RT-qPCR**

573 miRNA expression patterns identified by small RNA sequencing were validated with the
574 TaqMan MicroRNA Assay (Applied Biosystems). Reverse transcription was performed using
575 the TaqMan MicroRNA Reverse Transcription Kit (Applied Biosystems; CatNo. 4366596).

576 RT-qPCRs were conducted with the TaqMan Universal Master Mix II, no UNG (Applied
577 Biosystems; CatNo. 4440040) on a StepOnePlus Real-Time PCR System (Applied
578 Biosystems). The U6 snRNA was used as a control for normalization of experimental samples.
579 Relative quantification (RQ) values of miRNA expression were calculated with the ΔΔCT
580 method. Expression levels in NPCs and E14 samples, respectively, were used as reference
581 groups. Primers used for the RT-qPCR Analysis are shown in Additional file 1, Table S1.
582

583 **miRNA co-targeting prediction**

584 miRNA co-targeting analysis was performed using a custom R script. We employed the
585 TargetScanMouse database v7.2 to identify the broadly conserved mRNA targets for each
586 miRNA. miRNAs which belong to the same broadly conserved family and therefore have
587 identical gene target sets were grouped together for further analysis. Additionally, we only kept
588 miRNAs with at least 300 targets [20].
589 Subsequently, we created a custom control set for each miRNA, containing genes with similar
590 3' UTR length, GC content, and sequence conservation as the actual genes included in the
591 respective target set based on a case-control strategy. To select the best matching control for a
592 gene *X* from the respective target set (case), first we filtered the potential pool of candidates
593 for genes with a 3' UTR length within the range of 0.85-1.15 of the 3'UTR length of target
594 gene *X.* Then, we filtered out genes with a GC content outside the range of 0.95-1.05 of the
595 GC content of gene *X*. Finally, we eliminated candidates with a phyloP score outside the range
596 of 0.8-1.2 for gene *X.* If more than one candidate remained after the filtering steps, a control
597 gene *Y* for the target gene *X* was picked randomly. If the filtering steps returned an empty set,
598 no control gene was selected for the respective target. This procedure was repeated for all genes
599 included in the target set for the miRNA. The filtering cut-off values were selected empirically
600 to maximize the number of controls while simultaneously minimizing the difference in the 3'

601 UTR length, GC content, and phyloP score distributions of genes in the target and control sets.
602 The similarity of the distributions of the three parameters between the control and target sets
603 was ensured by non-significant pairwise Wilcoxon tests.
604 We considered miRNA *A* and miRNA *B* to be a co-targeting pair if the intersection of their
605 target sets contained more genes than what would be expected by chance. To this end, we
606 compared the observed number of common targets with the expected number obtained by
607 intersecting the target set of miRNA *A* with the control set of miRNA *B* and vice versa. This
608 yields two comparisons for each pair of miRNAs whose significance was evaluated with a
609 Fisher's exact test. If both tests were statistically significant after a false discovery rate p-value
610 adjustment (Benjamini-Hochberg method), then we considered miRNA *A* and miRNA *B* to be
611 a bidirectional co-targeting pair. To quantify the magnitude of the co-targeting relationship, we
612 calculated the odds ratios with values significantly higher than 1 corresponding to a pair of
613 miRNAs sharing a significantly higher number of targets than what would be expected by
614 chance. Higher odds ratios indicate a higher number of shared targets. To ensure that co-
615 targeting pairs do not originate from identical seed sequences, miRNAs having identical seeds
616 up to one mismatch were excluded *a priori* from the statistical analysis.
617
618 **Comparing the number of intra- and inter-modular co-targeting relationships**
619 To investigate if the black or green WCGNA modules contain more intra-modular (miRNAs
620 of the same module) than inter-modular (miRNAs from different modules) co-targeting
621 relationships, we performed a Fisher's exact test on the following contingency table:

	Significant co-targeting relationship	Non-significant co-targeting relationship
Intra-modular	m	M - m
Inter-modular	n	N - n

622 where m represents the number of significant intra-modular co-targeting relationships, M
623 corresponds to the total number of possible intra-modular relationships, n corresponds to the
624 number of significant inter-modular relationships and N refers to the total number of possible
625 inter-modular relationships. We used the following formula to calculate M:

626 $$M = x(x-1)/2$$

627 where x corresponds to the number of miRNAs in the respective module. The total number of
628 possible inter-modular relationships was estimated with the formula:

629 $$N = xy$$

630 with x being the number of miRNAs in the module of interest and y corresponding to the
631 number of miRNAs in the remaining modules.

632

633 **Luciferase reporter assays**

634 3' UTR fragments of miRNA target genes (for primer sequences see Additional File 1, Table
635 S2) were cloned into the XhoI/NotI sites downstream of the synthetic *Renilla* luciferase gene
636 of psiCHECK-2 vector (Promega; CatNo. C8021). Mutations in the miRNA binding sites were
637 introduced using the QuikChange II XL system (Agilent Technologies; CatNo. 200521-5).
638 Primers used are shown in Additional file 1, Table S2. $5x10^4$ HEK293 cells were seeded into
639 each well of a 12-well plate. 24 hours later, 200 ng psiCHECK-2 reporter plasmid were co-
640 transfected with 5 µl miScript miRNA mimics (Qiagen; CatNo. 219600) using 4 µl
641 Lipofectamine 2000 Transfection Reagent (Thermo Fisher Scientific; CatNo. 11668019).
642 Luciferase reporter assays were conducted 48 hours later using the Dual-Luciferase Reporter
643 Assay System (Promega; CatNo. E1980). Luciferase activity was measured on a CentroXS LB
644 960 (Berthold Technologies).

645

646 **Statistical analysis of qPCR and luciferase reporter assay data**

647 Two groups were compared statistically using an unpaired t-test or Welch's t-test in case of
648 unequal variance between groups. For comparisons of three groups, a one- or two-way analysis
649 of variance (ANOVA) followed by Tukey's post hoc test was performed. The assumptions of
650 the linear model were evaluated by inspecting Q-Q plots and fitted values vs. residuals plots.
651 Relative quantification values from the RT-qPCR assays were $\log_e$-transformed prior to
652 statistical testing. All p-values are two-tailed and a p-value ≤ 0.05 was considered statistically
653 significant. Statistical analysis was performed using R v. 4.2.2.
654

655 ## Declarations

656 **Ethics approval and consent to participate**

657 Ethical review and approval were not required for the animal study because the study did not
658 include any animal experiments requiring approval. To carry out this study, mice were killed
659 for organ removal. In Germany, this procedure is notifiable but does not require approval by
660 an ethics committee.

661 **Consent for publication**

662 Not applicable

663 **Availability of data and materials**

664 The raw RNA-seq data were uploaded to the Sequence Read Archive (SRA) data base under
665 the accession number PRJNA1018560.

666 The following supplementary tables are available online under 10.5281/zenodo.1016183:

667 Supplementary_table_1.xlsx: Differentially expressed miRNAs between E14, E17 and P0
668 cortical samples as well as NPCs versus neurons

669 Supplementary_table_2.xlsx: Module assignment of miRNAs in the WCGNA analysis.

670 Supplementary_table_3.xlsx: GO terms of miRNA targets of the black and green modules from
671 the WCGNA analysis.

Supplementary_table_4.xlsx: Significant co-targeting relationships between miRNAs/miRNA families.

Competing interests

The authors declare they have no competing interests.

Funding

HT and SG acknowledge funding by the Landesinitiative Rheinland-Pfalz and the Resilience, Adaptation, and Longevity (ReALity) initiative of the Johannes Gutenberg University of Mainz. SW was funded by the Emergent Algorithmic Intelligence initiative of the Johannes Gutenberg University Mainz supported by the Carl-Zeiss foundation. JW acknowledges funding from the Deutsche Forschungsgemeinschaft (WI-3837 / 8-1).

Authors' contributions

HT, DH and SW performed the bioinformatics analysis. LS and HM performed miRNA sequencing, RT-qPCR and luciferase experiments. HT and JW wrote the manuscript. SG and JW supervised the study. All authors read and approved the final version of the manuscript.

Acknowledgements

None

References

1. Lee Y, Kim M, Han J, Yeom KH, Lee S, Baek SH, Kim VN: **MicroRNA genes are transcribed by RNA polymerase II.** *EMBO J* 2004, **23:**4051-4060.
2. Borchert GM, Lanier W, Davidson BL: **RNA polymerase III transcribes human microRNAs.** *Nat Struct Mol Biol* 2006, **13:**1097-1101.
3. Denli AM, Tops BB, Plasterk RH, Ketting RF, Hannon GJ: **Processing of primary microRNAs by the Microprocessor complex.** *Nature* 2004, **432:**231-235.
4. Gregory RI, Yan KP, Amuthan G, Chendrimada T, Doratotaj B, Cooch N, Shiekhattar R: **The Microprocessor complex mediates the genesis of microRNAs.** *Nature* 2004, **432:**235-240.
5. Han J, Lee Y, Yeom KH, Kim YK, Jin H, Kim VN: **The Drosha-DGCR8 complex in primary microRNA processing.** *Genes Dev* 2004, **18:**3016-3027.
6. Yi R, Qin Y, Macara IG, Cullen BR: **Exportin-5 mediates the nuclear export of pre-microRNAs and short hairpin RNAs.** *Genes Dev* 2003, **17:**3011-3016.

702 7. Ketting RF, Fischer SE, Bernstein E, Sijen T, Hannon GJ, Plasterk RH: **Dicer functions**
703 **in RNA interference and in synthesis of small RNA involved in developmental**
704 **timing in C. elegans.** *Genes Dev* 2001, **15:**2654-2659.
705 8. O'Brien J, Hayder H, Zayed Y, Peng C: **Overview of MicroRNA Biogenesis,**
706 **Mechanisms of Actions, and Circulation.** *Front Endocrinol (Lausanne)* 2018, **9:**402.
707 9. Davis TH, Cuellar TL, Koch SM, Barker AJ, Harfe BD, McManus MT, Ullian EM:
708 **Conditional loss of Dicer disrupts cellular and tissue morphogenesis in the cortex**
709 **and hippocampus.** *J Neurosci* 2008, **28:**4322-4330.
710 10. McLoughlin HS, Fineberg SK, Ghosh LL, Tecedor L, Davidson BL: **Dicer is required for**
711 **proliferation, viability, migration and differentiation in corticoneurogenesis.**
712 *Neuroscience* 2012, **223:**285-295.
713 11. Kawase-Koga Y, Otaegi G, Sun T: **Different timings of Dicer deletion affect**
714 **neurogenesis and gliogenesis in the developing mouse central nervous system.** *Dev*
715 *Dyn* 2009, **238:**2800-2812.
716 12. Nowakowski TJ, Mysiak KS, Pratt T, Price DJ: **Functional dicer is necessary for**
717 **appropriate specification of radial glia during early development of mouse**
718 **telencephalon.** *PLoS One* 2011, **6:**e23013.
719 13. Saurat N, Andersson T, Vasistha NA, Molnar Z, Livesey FJ: **Dicer is required for neural**
720 **stem cell multipotency and lineage progression during cerebral cortex**
721 **development.** *Neural Dev* 2013, **8:**14.
722 14. De Pietri Tonelli D, Pulvers JN, Haffner C, Murchison EP, Hannon GJ, Huttner WB:
723 **miRNAs are essential for survival and differentiation of newborn neurons but not**
724 **for expansion of neural progenitors during early neurogenesis in the mouse**
725 **embryonic neocortex.** *Development* 2008, **135:**3911-3921.
726 15. De Pietri Tonelli D, Clovis YM, Huttner WB: **Detection and monitoring of microRNA**
727 **expression in developing mouse brain and fixed brain cryosections.** *Methods Mol*
728 *Biol* 2014, **1092:**31-42.
729 16. Alles J, Fehlmann T, Fischer U, Backes C, Galata V, Minet M, Hart M, Abu-Halima M,
730 Grasser FA, Lenhof HP, et al: **An estimate of the total number of true human**
731 **miRNAs.** *Nucleic Acids Res* 2019, **47:**3353-3364.
732 17. Prieto-Colomina A, Fernández V, Chinnappa K, Borrell V: **MiRNAs in early brain**
733 **development and pediatric cancer: At the intersection between healthy and**
734 **diseased embryonic development.** *Bioessays* 2021, **43:**e2100073.
735 18. Winter J: **MicroRNAs of the miR379-410 cluster: New players in embryonic**
736 **neurogenesis and regulators of neuronal function.** *Neurogenesis (Austin)* 2015,
737 **2:**e1004970.
738 19. Rago L, Beattie R, Taylor V, Winter J: **miR379-410 cluster miRNAs regulate**
739 **neurogenesis and neuronal migration by fine-tuning N-cadherin.** *EMBO J* 2014,
740 **33:**906-920.
741 20. Cherone JM, Jorgji V, Burge CB: **Cotargeting among microRNAs in the brain.** *Genome*
742 *Res* 2019, **29:**1791-1804.
743 21. Krek A, Grun D, Poy MN, Wolf R, Rosenberg L, Epstein EJ, MacMenamin P, da
744 Piedade I, Gunsalus KC, Stoffel M, Rajewsky N: **Combinatorial microRNA target**
745 **predictions.** *Nat Genet* 2005, **37:**495-500.
746 22. Nielsen CB, Shomron N, Sandberg R, Hornstein E, Kitzman J, Burge CB: **Determinants**
747 **of targeting by endogenous and exogenous microRNAs and siRNAs.** *RNA* 2007,
748 **13:**1894-1910.

749 23. Grimson A, Farh KK, Johnston WK, Garrett-Engele P, Lim LP, Bartel DP: **MicroRNA**
750 **targeting specificity in mammals: determinants beyond seed pairing.** *Mol Cell* 2007,
751 **27:**91-105.
752 24. Saetrom P, Heale BS, Snove O, Jr., Aagaard L, Alluin J, Rossi JJ: **Distance constraints**
753 **between microRNA target sites dictate efficacy and cooperativity.** *Nucleic Acids Res*
754 2007, **35:**2333-2342.
755 25. Doench JG, Sharp PA: **Specificity of microRNA target selection in translational**
756 **repression.** *Genes Dev* 2004, **18:**504-511.
757 26. Wu S, Huang S, Ding J, Zhao Y, Liang L, Liu T, Zhan R, He X: **Multiple microRNAs**
758 **modulate p21Cip1/Waf1 expression by directly targeting its 3' untranslated region.**
759 *Oncogene* 2010, **29:**2302-2308.
760 27. Loo L, Simon JM, Xing L, McCoy ES, Niehaus JK, Guo J, Anton ES, Zylka MJ: **Single-cell**
761 **transcriptomic analysis of mouse neocortical development.** *Nature*
762 *Communications* 2019, **10:**134.
763 28. Mukhtar T, Taylor V: **Untangling Cortical Complexity During Development.** *Journal*
764 *of Experimental Neuroscience* 2018, **12:**1179069518759332.
765 29. Ling K-H, Brautigan PJ, Hahn CN, Daish T, Rayner JR, Cheah P-S, Raison JM, Piltz S,
766 Mann JR, Mattiske DM, et al: **Deep sequencing analysis of the developing mouse**
767 **brain reveals a novel microRNA.** *BMC Genomics* 2011, **12:**176.
768 30. Cadwell CR, Bhaduri A, Mostajo-Radji MA, Keefe MG, Nowakowski TJ: **Development**
769 **and Arealization of the Cerebral Cortex.** *Neuron* 2019, **103:**980-1004.
770 31. Bagot RC, Cates HM, Purushothaman I, Lorsch ZS, Walker DM, Wang J, Huang X,
771 Schlüter OM, Maze I, Peña CJ, et al: **Circuit-wide Transcriptional Profiling Reveals**
772 **Brain Region-Specific Gene Networks Regulating Depression Susceptibility.** *Neuron*
773 2016, **90:**969-983.
774 32. Lorsch ZS, Hamilton PJ, Ramakrishnan A, Parise EM, Salery M, Wright WJ, Lepack AE,
775 Mews P, Issler O, McKenzie A, et al: **Stress resilience is promoted by a Zfp189-driven**
776 **transcriptional network in prefrontal cortex.** *Nature Neuroscience* 2019, **22:**1413-
777 1423.
778 33. Langfelder P, Horvath S: **WGCNA: an R package for weighted correlation network**
779 **analysis.** *BMC Bioinformatics* 2008, **9:**559.
780 34. Weyn-Vanhentenryck SM, Feng H, Ustianenko D, Duffié R, Yan Q, Jacko M, Martinez
781 JC, Goodwin M, Zhang X, Hengst U, et al: **Precise temporal regulation of alternative**
782 **splicing during neural development.** *Nature Communications* 2018, **9:**2189.
783 35. Huang HY, Lin YC, Cui S, Huang Y, Tang Y, Xu J, Bao J, Li Y, Wen J, Zuo H, et al:
784 **miRTarBase update 2022: an informative resource for experimentally validated**
785 **miRNA-target interactions.** *Nucleic Acids Res* 2022, **50:**D222-d230.
786 36. Zhang X, Chen MH, Wu X, Kodani A, Fan J, Doan R, Ozawa M, Ma J, Yoshida N, Reiter
787 JF, et al: **Cell-Type-Specific Alternative Splicing Governs Cell Fate in the Developing**
788 **Cerebral Cortex.** *Cell* 2016, **166:**1147-1162.e1115.
789 37. Zhang M, Ergin V, Lin L, Stork C, Chen L, Zheng S: **Axonogenesis Is Coordinated by**
790 **Neuron-Specific Alternative Splicing Programming and Splicing Regulator PTBP2.**
791 *Neuron* 2019, **101:**690-706.e610.
792 38. Lin YS, Wang HY, Huang DF, Hsieh PF, Lin MY, Chou CH, Wu IJ, Huang GJ, Gau SS,
793 Huang HS: **Neuronal Splicing Regulator RBFOX3 (NeuN) Regulates Adult**
794 **Hippocampal Neurogenesis and Synaptogenesis.** *PLoS One* 2016, **11:**e0164164.

795 39. Makeyev EV, Zhang J, Carrasco MA, Maniatis T: **The MicroRNA miR-124 promotes**
796 **neuronal differentiation by triggering brain-specific alternative pre-mRNA splicing.**
797 *Mol Cell* 2007, **27:**435-448.
798 40. Jensen KB, Dredge BK, Stefani G, Zhong R, Buckanovich RJ, Okano HJ, Yang YY,
799 Darnell RB: **Nova-1 regulates neuron-specific alternative splicing and is essential for**
800 **neuronal viability.** *Neuron* 2000, **25:**359-371.
801 41. Ule J, Ule A, Spencer J, Williams A, Hu JS, Cline M, Wang H, Clark T, Fraser C, Ruggiu
802 M, et al: **Nova regulates brain-specific splicing to shape the synapse.** *Nat Genet*
803 2005, **37:**844-852.
804 42. Tutukova S, Tarabykin V, Hernandez-Miranda LR: **The Role of Neurod Genes in Brain**
805 **Development, Function, and Disease.** *Frontiers in Molecular Neuroscience* 2021, **14**.
806 43. Wang JT, Song LZ, Li LL, Zhang W, Chai XJ, An L, Chen SL, Frotscher M, Zhao ST: **Src**
807 **controls neuronal migration by regulating the activity of FAK and cofilin.**
808 *Neuroscience* 2015, **292:**90-100.
809 44. Li M, Ransohoff RM: **Multiple roles of chemokine CXCL12 in the central nervous**
810 **system: a migration from immunology to neurobiology.** *Prog Neurobiol* 2008,
811 **84:**116-131.
812 45. Mithal DS, Banisadr G, Miller RJ: **CXCL12 signaling in the development of the**
813 **nervous system.** *J Neuroimmune Pharmacol* 2012, **7:**820-834.
814 46. Dori M, Cavalli D, Lesche M, Massalini S, Alieh LHA, de Toledo BC, Khudayberdiev S,
815 Schratt G, Dahl A, Calegari F: **MicroRNA profiling of mouse cortical progenitors and**
816 **neurons reveals miR-486-5p as a regulator of neurogenesis.** *Development* 2020,
817 **147**.
818 47. Shu P, Wu C, Liu W, Ruan X, Liu C, Hou L, Zeng Y, Fu H, Wang M, Chen P, et al: **The**
819 **spatiotemporal expression pattern of microRNAs in the developing mouse nervous**
820 **system.** *Journal of Biological Chemistry* 2019, **294:**3444-3453.
821 48. Pilaz L-J, Silver DL: **Post-transcriptional regulation in corticogenesis: how RNA-**
822 **binding proteins help build the brain.** *WIREs RNA* 2015, **6:**501-515.
823 49. Mukhtar T, Breda J, Adam MA, Boareto M, Grobecker P, Karimaddini Z, Grison A,
824 Eschbach K, Chandrasekhar R, Vermeul S, et al: **Temporal and sequential**
825 **transcriptional dynamics define lineage shifts in corticogenesis.** *Embo j* 2022,
826 **41:**e111132.
827 50. Telley L, Govindan S, Prados J, Stevant I, Nef S, Dermitzakis E, Dayer A, Jabaudon D:
828 **Sequential transcriptional waves direct the differentiation of newborn neurons in**
829 **the mouse neocortex.** *Science* 2016, **351:**1443-1446.
830 51. Nowakowski TJ, Rani N, Golkaram M, Zhou HR, Alvarado B, Huch K, West JA, Leyrat
831 A, Pollen AA, Kriegstein AR, et al: **Regulation of cell-type-specific transcriptomes by**
832 **microRNA networks during human brain development.** *Nature Neuroscience* 2018,
833 **21:**1784-1792.
834 52. Graham V, Khudyakov J, Ellis P, Pevny L: **SOX2 Functions to Maintain Neural**
835 **Progenitor Identity.** *Neuron* 2003, **39:**749-765.
836 53. Hagey DW, Muhr J: **Sox2 Acts in a Dose-Dependent Fashion to Regulate**
837 **Proliferation of Cortical Progenitors.** *Cell Reports* 2014, **9:**1908-1920.
838 54. Stevanovic M, Stanisavljevic Ninkovic D, Mojsin M, Drakulic D, Schwirtlich M:
839 **Interplay of SOX transcription factors and microRNAs in the brain under**
840 **physiological and pathological conditions.** *Neural Regen Res* 2022, **17:**2325-2334.

841 55. Bian S, Hong J, Li Q, Schebelle L, Pollock A, Knauss JL, Garg V, Sun T: **MicroRNA**
842 **cluster miR-17-92 regulates neural stem cell expansion and transition to**
843 **intermediate progenitors in the developing mouse neocortex.** *Cell Rep* 2013,
844 **3:**1398-1406.
845 56. Sun G, Ye P, Murai K, Lang MF, Li S, Zhang H, Li W, Fu C, Yin J, Wang A, et al: **miR-137**
846 **forms a regulatory loop with nuclear receptor TLX and LSD1 in neural stem cells.**
847 *Nat Commun* 2011, **2:**529.
848 57. Vuong CK, Black DL, Zheng S: **The neurogenetics of alternative splicing.** *Nature*
849 *Reviews Neuroscience* 2016, **17:**265-281.
850 58. Linsen SEV, Tops BBJ, Cuppen E: **miRNAs: small changes, widespread effects.** *Cell*
851 *Research* 2008, **18:**1157-1159.
852 59. Ramsköld D, Wang ET, Burge CB, Sandberg R: **An abundance of ubiquitously**
853 **expressed genes revealed by tissue transcriptome sequence data.** *PLoS Comput Biol*
854 2009, **5:**e1000598.
855 60. Miura P, Shenker S, Andreu-Agullo C, Westholm JO, Lai EC: **Widespread and**
856 **extensive lengthening of 3' UTRs in the mammalian brain.** *Genome Res* 2013,
857 **23:**812-825.
858 61. Agarwal V, Bell GW, Nam J-W, Bartel DP: **Predicting effective microRNA target sites**
859 **in mammalian mRNAs.** *eLife* 2015, **4:**e05005.
860 62. Margolin AA, Nemenman I, Basso K, Wiggins C, Stolovitzky G, Favera RD, Califano A:
861 **ARACNE: An Algorithm for the Reconstruction of Gene Regulatory Networks in a**
862 **Mammalian Cellular Context.** *BMC Bioinformatics* 2006, **7:**S7.
863